

On the role of preflares in tornado-type prominences

Yu.A. Kupryakov^{1,2,*}, P. Kotrč¹, L.K. Kashapova³

¹*Astronomical Institute AS CR, Ondřejov, Czech Republic*

²*Sternberg Astronomical Institute (Lomonosov Moscow University), Russia*

³*Institute of Solar-Terrestrial Physics SB RAS, 6640333 Irkutsk, Russia*

Received 1 October, 2018

We present first results of a study of rotation parameters of the tornado-type prominences using H α line spectra and filtergrams. The prominences of the tornado-type were observed by ground-based spectrographs MFS and HSFA 2 in the Ondřejov Observatory (Astronomical Institute of AS CR) from 2000 to 2017. The analysis took into account the structure and dynamics of selected prominences and a comparison of the data of H α with the EUV observations of SDO (304 Å, 193 Å, 171 Å), as well as information about the emission of flares in the X-ray range. We found that most of the analyzed events were associated with solar flares of classes from B5 to M5 by GOES classification. We revealed two types of motions in the prominences. The first type shows the Doppler velocity quasi-symmetry of the values in the “blue” and “red” H α line wings. The events of the other type demonstrate a difference of up to one order of velocities in the direction of, and towards, the observer.

Keywords: Prominences, solar flare

1 Introduction

There is a distinguished group among active prominences, the motion of which looks like an earth tornado (Wedemeyer-Böhm et al., 2012). At the present time, these mysterious objects are actively being investigated by observations in the extra ultra-violet (EUV) range. This type relates to instability of hosting prominence and it is considered as a possible precursor of various eruptions from jets to the Coronal Mass Ejections (see the most recent publications by Mghebrishvili et al., 2018; Chen et al., 2017). Information about the motion of matter in solar prominences as a marker of their activity can be obtained from spectral observations only. EUV spectral observations provide information about hot plasma (see Levens et al. 2017). The H α observation contains information about behaviours of cool plasma. The results of

*Email: kupry@asu.cas.cz

studies by Schmieder et al. (2017) showed that the Doppler pattern observed in $H\alpha$ cannot be interpreted as rotation of the cool plasma inside the tornado. This fact needs additional observational data that could be obtained during new observational campaigns or found in the already existing databases. The aim of this study was to select the tornado-type prominences and carry out preliminary analysis of their Doppler velocities and relationship with solar flare onsets.

2 Observations: Data and analysis

The $H\alpha$ observation of the prominence we took from the morphological catalogue of prominences compiled from observations on the horizontal solar spectrographs: MFS, Multichannel-Flare-Spectrograph; SLS, Solar Laboratory Spectrograph; and HSFA-2, Horizontal-Sonnen-Forschungs-Anlage 2. These instruments are located on the Ondřejov Observatory of the Astronomical Institute of the Academy of Sciences of the Czech Republic near Prague. The MFS spectrograph was built in the 1950s (Valníček et al., 1959) and reconstructed in 1990 (Kotrč et al., 1992). The regular observations on it started in 1996. The solar spectrograph (HSFA-2), manufactured by Carl Zeiss, was installed at the observatory in the late 1980s. After modernization in 2004 (Kotrč, 2008), it is possible to obtain spectra in five selected spectral lines simultaneously and also to get images of the chromosphere on the slit of the spectrograph in the line $H\alpha$ (Kotrč et al., 2007).

Selecting the prominences for the catalogue, we also used observations by the Atmospheric Imaging Assembly on board of the Solar Dynamic Observatory (Lemen et al., 2012) in lines 304 Å, 193 Å, 171 Å. The main criteria for selection are the intensity of radiation in the spectral lines Ca II (H, K), $H\beta$, D 3, Mg I (5167.327, 5172.698 Å), $H\alpha$, CaIR 8542 Å, the structure seen in the lines of $H\alpha$, He II and 193 Å, the presence of visible motions in the prominence; the structure of the velocity field. An example of spectral data is shown in Fig. 1. To identify and detail the objects, we used observation bases: Kanzelhöhe Observatory, BASS2000, Solar Activity Monitoring and Forecasting.

Table 1 presents the selected events and their parameters. The first column is the observation date, the second is time. The fourth column presents the Doppler

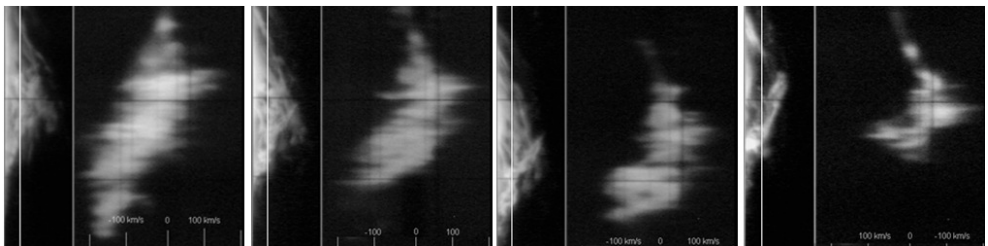


Figure 1 The MFS observation of the prominence taken on 12 June 2003 at 14:24:48, 14:29:32, 14:32:21 and 14:38:53 UT from left to right. The image is composed of $H\alpha$ filtergram (left parts) and $H\alpha$ spectrogram. The white vertical line corresponds to the position of the slit of the spectrograph. At the bottom of the picture is a scale of Doppler velocities.

Table 1 Tornado-type prominences observed in 2001–2017. The columns show the date and time of observation, Doppler velocity in the line $H\alpha$ in km/s, presence and GOES class of solar flares related to the event, position of the event on eastern (E) or western (W) limb, presence of emission in the line Mg I marked by (*) symbol.

Date	Time	Velocity [km/s]	GOES class	Position
2001-05-09	04:57–11:37	+150, –120	C2 (09:00)	E
2001-05-20	05:58–10:51	+200, –200	M1 (09:30)	W
2002-06-26	05:47–09:00	+60, –90	B8 (08:10)	E
2002-08-04	09:01–09:47	+200, –250	M5 (09:15)	E
2003-06-12	14:19–14:41	+190, –100	C2.9(14:47)	W
2003-08-01	10:20–10:40	+200, –100	B5 (10:23)	W
2004-04-23	05:58–12:13	+115, –110	M1 (12:00)	W
2011-06-25	06:33–13:53	+41, –18	B6 (10:20)	E
2012-05-10	07:13–09:06	+11, –10	C1 (07:30)	E
2012-05-20	05:18–13:48	+9, –25	B9 (10:10)	E
2012-05-25	05:36–10:47	+10, –13	C1 (10:15)	W
2012-05-26	05:41–08:18	+8, –11	B8 (06:05)	W
2012-06-11	13:10–13:20	+182, –12		W
2012-06-21	07:05–09:23	+5, –24		W
2014-03-30	06:51–11:15	+22, –27		E
2014-04-12	07:16–07:51	+100, –150	C5.0(07:15)	E
2014-04-19	09:32–09:42	+75, –80		W
2014-04-23	11:10–12:09	+230, –130	M1.5(11:50)	W
2014-05-23	07:08–07:50	+15, –10		W
2015-04-15	12:58–13:07	+5, –7		E
2015-04-21	12:58–13:50	+100, –140		E*
2015-05-24	06:21–06:52	+3, –2		E*
2015-10-02	05:44–13:02	+80, –75	C4(08:50)	W
2016-04-03	06:21–14:55	+4, –3	B3(13:40)	W
2017-05-01	06:15–12:33	+5, –4	B1.4(09:11)	W*

velocities in km/s. The positive sign means red wing velocity and the negative is blue wing velocity. In our analysis, we paid special attention to tornado-type prominences related to solar flares that occurred near them or flares that occurred in prominences during their evolution. Thus, the fifth column presents the GOES class of such a flare and its maximum time. The sixth column shows the position of the prominence – western or eastern limb. We present three events as an example of the evolution of prominences and subsequent solar flares. Positions of X-ray sources were reconstructed using RHESSI observations and software (Lin et al., 2002). In the case of AIA/SDO observations, we used available images in EUV by EIT/SOHO.

The first event is the prominence observed on 12 June 2003 ($X = 929''$, $Y = 203''$) in the NOAA 10375. One can see in Fig. 1 the evolution of a fine rotating structure to a more compact structure, which resulted in a C2.9 GOES class flare (14:47 UT) (see Fig. 4a).

The $H\alpha$ spectral observations of the prominence developing on 23 April 2004 ($X = 967''$, $Y = -130''$) are shown in Fig. 2. This prominence initiated several faint flares during the evolution. We showed the first flare in Fig. 4b. The development of the

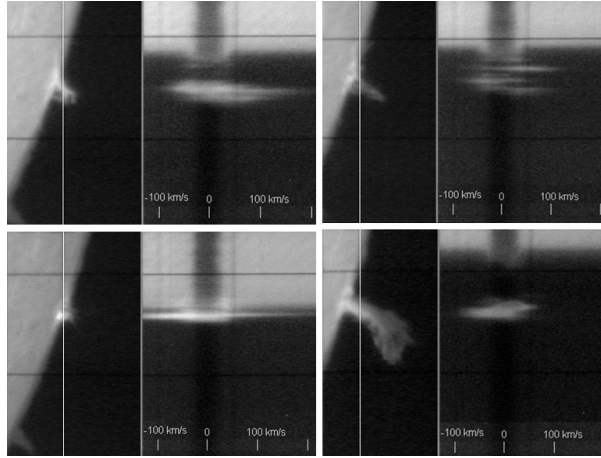


Figure 2 The MFS observation of the prominence taken on 23 April 2004 at 11:10:01, 11:21:27, 11:47:26 and 12:09:37 UT from left to right. The image is composed of $H\alpha$ filtergram and $H\alpha$ spectrogram. The white vertical line corresponds to the position of the slit of the spectrograph. At the bottom of the picture is a scale of Doppler velocities.

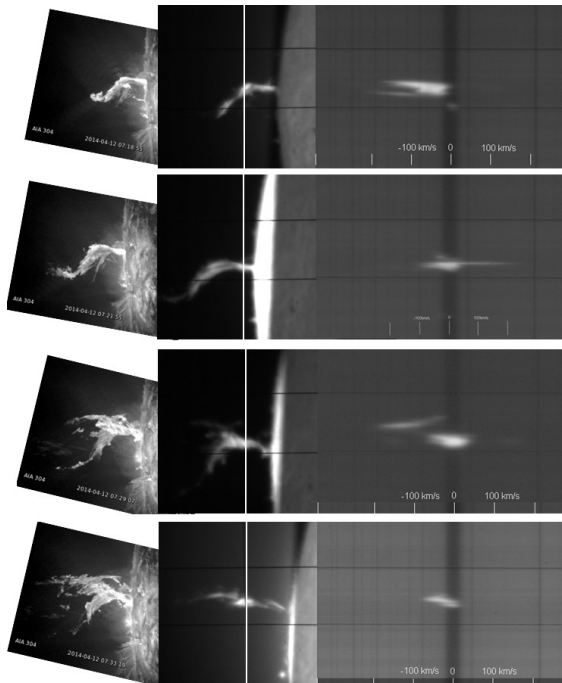


Figure 3 For April 12, 2014 from top down: SDO images 304 Å; the MFS observation of the prominence taken at 07:19:08, 07:21:49, 07:28:55 and 07:49:26 UT. The image MFS is composed of $H\alpha$ filtergram (left parts) and $H\alpha$ spectrogram. The white vertical line corresponds to the position of the slit of the spectrograph. At the bottom of the picture is a scale of Doppler velocities.

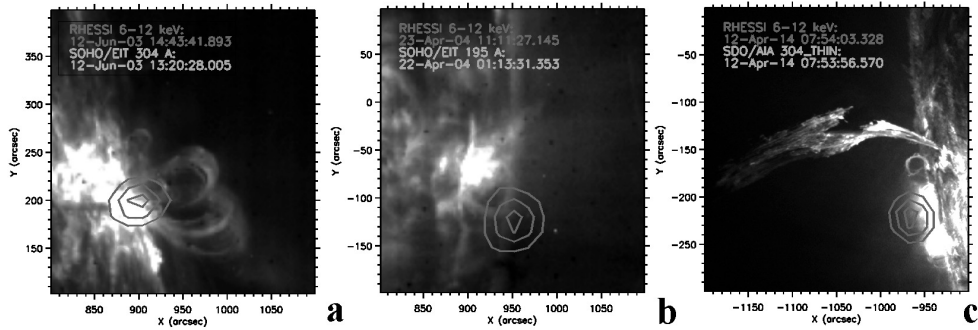


Figure 4 The position of the isodense X-ray source (RHESSI 6–12 keV) is superimposed on the image of the region in the line 304 Å: a) 12 June 2003 at 14:43:41 UT; b) 23 April 2004 at 11:11:27 UT; c) 12 April 2014 at 07:54:03 UT.

the spinning of the spindle-shaped structure resulted in a sufficiently powerful M1.0 GOES class flare which occurred at 11:41 UT.

The last shown event turned out on 12 April 2014 ($X = -942''$, $Y = -256''$) in Fig. 3. It can be clearly seen that the limb C5.0 flare (07:15 UT) and the prominence were closely located in the same active region (see Fig. 4c). It is interesting that the flare preceded the formation and evolution of tornado.

3 Summary

We revealed 25 tornado-type events in observations carried out during 2001–2017. The number of the events which took place on the Eastern and Western limbs is equal. We found that most of the selected events were temporally and spatially associated with the onsets of the solar flares. The GOES class of these flares varied from B5 to M5. Probably the events without the consequence of flare arising were the result of projection effect. But it needs a further study. The Doppler velocities were within 2–200 km/sec for both directions. We can separate the observed events into two subtypes. The first type of events shows the quasi-symmetry of the Doppler velocities in the “blue” and “red” velocity. Events of the other subtype demonstrate a significant difference of the velocity values. Sometimes it can rise up to a factor of 10. We noted that the events with very significant asymmetry were not related to flare onset. Most probably it could be an indicator of tornado-type seen because of the projection effect. Surely this fact could be explained by the orientation of the rotation plane relative to the line-of-sight but it should be studied by reconstruction of this parameter in 3D coordinates.

Acknowledgements

P.K. and Yu.A.K. appreciate a support from Grant GACR No. 16-18495S.

References

- Chen, H., Zhang, J., Ma, S. et al., 2017, *The Astrophysical Journal Letters*, 841, 1
- Kotrč, P., Heinzl P. and Knížek, M., 1993, *JOSO annual Report 1992*, 144
- Kotrč, P., 2008, *Cent. Eur. Astrophys. Bull.* 1, 1
- Kotrč, P., Kononovich, E.V. and Kupryakov, Yu.A., 2007, *Astronomical and Astrophysical Transactions*, V. 26, pp. 267–273
- Lin, R.P., Dennis, B.R., Hurford, G.J. et al., 2002, *Solar Phys.*, 210, pp. 3–32
- Lemen, J.R., Title, A.M., Akin, D.J. et al., 2012, *Solar Phys.*, 275, pp. 17–40
- Levens, P.J., Labrosse, N., Schmieder, B. et al., 2017, *Astronomy & Astrophysics*, 607, id. A16
- Mghebrishvili, I., Zaqarashvili, T.V., Kukhianidze, V. et al., 2018, *The Astrophysical Journal*, 861, 10
- Schmieder, B., Mein, P., Mein, N. et al, 2017, *Astronomy & Astrophysics*, 597, id. A109
- Valníček, B., Letfus, V., Blaha, M., Švestka, Z. and Seidl, Z., 1959, *Bull. Astron. Inst. Czechosl.* V. 10, p. 149
- Wedemeyer-Böhm, S., Scullion, E., Steiner, O. et al., 2012, *Nature*, 486, pp. 505–508